

¹ Estimating the dynamics of Ghanaian mangrove cover using
² phenological metrics derived from synoptic Landsat observations

³ Issoufou Liman Harou^{a,b,*}, Julliet Inyele^c, Peter Minang^a, Lalisa Duguma^a

^a*Governance and Landscapes World Agroforestry (ICRAF) UN Avenue Gigiri Nairobi Kenya P.O. Box:
30677-00100*

^b*Department of Environmental Sciences Kenyatta University Kenya Drive Nairobi Kenya P.O. Box:
43844-00100*

^c*Department of Geography Kenyatta University Kenya Drive Nairobi Kenya P.O. Box: 43844-00100*

⁴ **Abstract**

Remote sensing analysis and narratives from Ghana (West Africa) reported evidence of mangrove degradation across the southern regions of the country. Despite the importance of mangrove forests, the coverage of earth observation satellites and the recent advances in computing power for processing spatial data, spatially-explicit estimates of mangrove vegetation cover are lacking. In these regions, optical sensors onboard Landsat satellites provide a great deal of historical remote sensing data for studying land surface dynamics. While these sensors provide reasonable spatial, temporal and spectral resolutions for studying the dynamics of mangrove vegetation cover, a number of remote sensing artifacts make it difficult to derive a complete land cover map. In particular, the persistence of cloud cover limits the number of usable images. To understand the dynamics of mangrove forests, we identified 17 land cover classes, harmonized the Landsat scenes across sensors, used time series analysis to improve cloud detection and recover the relevant signal encoding the temporal signature of land cover. Based on the seasonal behavior of the land cover classes, the persistence of cloud cover limiting the number of usable images and the temporal resolution of Landsat satellite, we mosaiced the images within 30 days of their acquisition dates. Using the fitted image time series, we computed unsupervised classifications which we used along with ground control polygons to generate training and validation data for land cover classifications and change detection. The analysis of the root mean square error indicates that the accuracy of the fitted image time series increases with band wavelength and land cover seasonality. The accuracy assessment

indicates an overall accuracy between 0.94 and 0.95 and a Kappa between 0.93 and 0.95 for the different land cover classifications. Mangrove forests have declined in some areas, whereas they have increased in others. Mangrove area, which has decreased between 2000 and 2010, has increased between 2010 and 2020. The gains experienced between 2010 and 2020, however, did not compensate for the lost the land cover experienced between 2000 and 2010. We identified four top most important land cover involved in mangroves conversion including forests with a high rate, croplands and natural vegetation mosaics and tree plantations with moderate rate and wetlands with a low rate. Better mangrove restoration and conservation are required to fully reverse the trend of mangrove decline.

⁵ *Keywords:* Cloud Mask, Google Earth Engine, Landsat Data, Land Cover

⁶ Classification, Mangrove

⁷ Software and data availability

⁸ We conducted the data analysis in Google Earth Engine cloud computing platform
⁹ ([Gorelick et al., 2017](#)) and R programming language ([R Core Team, 2021](#)). These were
¹⁰ interfaced using rgee R package ([Aybar et al., 2020](#)) which we used as bridge for through-
¹¹ put between Google Earth engine and R. Both Google Earth engine and R are freely
¹² accessible (see <https://cran.r-project.org/index.html> for R and <https://code.earthengine.google.com/> for Google Earth Engine). We automated the entire process,
¹⁴ including the installation of the required R packages; data processing; data streaming
¹⁵ between Google Earth Engine and R; and results visualization, to provide a complete re-
¹⁶ producible workflow. The replication files along with further information for reproducing
¹⁷ the work are available from <https://github.com/Issoufou-Liman/mangrove-RSE>.

¹⁸ Definition of key terms

¹⁹ In this section, we define several terms which may lead to confusion. Remote sens-
²⁰ ing artifacts regroup all atmospheric (e.g., such as cloud, cloud shadow, haze, aerosol

*Corresponding author

Email addresses: issoufoul@gmail.com (Issoufou Liman Harou), inyelejuli@gmail.com (Julliet Inyele), A.Minang@cgiar.org (Peter Minang), l.duguma@cgiar.org (Lalisa Duguma)

scattering) and technical factors (e.g., scan line corrector failure in Landsat 7 Enhanced Thematic Mapper Plus) that would potentially lead to unrealistic pixel value estimates. The term “clear” (as in clear pixels or clear observation) refers to pixels exempt of remote sensing artifacts as estimated by Fmask algorithm. We used the term “cloudy” (as in cloudy observations or cloudy pixels) to denote pixel value identified by Fmask algorithm as affected by remote sensing artifacts. These are different from “noisy” (as in noisy observations). Noisy pixels are clear pixels whose values are not reasonably within the range of valid values. These are mostly cloudy pixels not identified by Fmask algorithm. We used the term “signal” to denote the smooth temporal distribution of pixel values that describes the average phenological profile at the pixel. This is smooth data describing the phenology of LULC and the information of interest as opposed to “noise” which denotes the random fluctuations that obscures the signal. We used the term “overall study period” to denote the period 2000 to 2020, the term “previous decade” to denote the period 2000 to 2010, and the term “last decade” to denote the period 2010 to 2020.

1. Introduction

Mangroves are coastal forests that grow where ocean water, freshwater, and land meet (CILSS, 2016). They are highly productive forest ecosystems found in the intertidal zone of tropical and subtropical coasts (Spalding et al., 1997, 2010; Wang et al., 2019). Mangrove trees develop adaptation mechanisms that enable them to survive in brackish water conditions (Spalding et al., 1997, 2010). They play important roles in regulating coastal processes, in providing various ecosystem services to the socio-ecological systems in the coastal regions, or in underpinning traditional customs for many communities (Ajonina et al., 2013; Levy et al., 2015; UNEP, 2007; Wilkie and Fortuna, 2003).

Recent studies (Rubin et al., 1999; Wilkie and Fortuna, 2003) estimated mangroves to cover between 14 and 17 million hectares of tropical coasts. Around 3.2 million ha of these (19% of global coverage) are found in Africa (Ajonina et al., 2013), with West Africa hosting 70% of the total mangrove areas of the continent (UNEP, 2007). In Ghana, the area covered by mangroves is estimated to range between 137 to 140 km² (Armah et al.,

49 2009; UNEP, 2007). Mangroves provide a substantial contribution to coastal fisheries,
50 which contribute to around \$400 million per year to the regional economy of West Africa
51 (USGS EROS, 2021). In Ghana, this value is estimated at \$6 million per year (Armah
52 et al., 2009).

53 Despite the importance of mangroves, some studies reported that mangrove vegetation
54 cover has been alarmingly declining in many areas of Ghana for the last few decades
55 (Asante et al., 2017). Armah et al. (2009) estimated this decline to range between 20 and
56 30% across the coast of Atlantic Ocean over the past 3 decades. FAO (2007) reported
57 a mangrove vegetation loss of 0.5 million ha (13.8 % of the total mangrove areas) in 25
58 years. According to Rubin et al. (1999), almost 2/3 of the Volta estuary mangroves have
59 been lost since 1973, leaving only a few patches within a buffer of 15 km. Darkwa and
60 Smardon (2010) noticed an increased cutting of mangroves vegetation in Fosu Lagoon.
61 FAO (2007) estimated the decline of mangrove areas in Ghana at 24% between 1980 to
62 2005. In other areas, however, other studies reported an appreciable increase in mangrove
63 vegetation cover following restoration efforts by the locals. Awo et al. (2014) reported a
64 noticeable increase in mangrove cover between 1986 and 2002 in Anyanui (Keta Lagoon).
65 Feka (2015) noted that despite the reduction in mangrove area in Ghana, an estimated
66 area of 68 ha of mangroves have been restored from 1980 to 2006.

67 It becomes clear from the available information that a country-wide assessment of
68 mangrove vegetation in Ghana is needed. A holistic assessment of all major Land Use
69 Land Cover (LULC) would help to understand the dynamics of mangrove vegetation and
70 guide mangrove conservation policy in the study area. This would help identify areas
71 of increase and decrease in mangrove vegetation, understand the trend in LULC change,
72 identify areas that require immediate action and those areas where policy interventions
73 can achieve the greatest impact. To our knowledge, country-wide assessments of mangrove
74 vegetation that deliver this crucial information for mangrove conservation are lacking. The
75 most recent and comprehensive ones (e.g., CILSS (2016); Spalding et al. (1997); Spalding
76 et al. (2010)) have either coarse spatial resolution or have important information gap to
77 be suitable for this purpose. This information gap is mainly due to the prevalence of cloud

78 cover ([Ashiagbor et al., 2021](#)) that makes it virtually impossible to derive a complete land
79 cover map from a single acquisition ([Rubin et al., 1999](#)). Clouds deserved a standalone
80 class in [CILSS \(2016\)](#) because none of the best available image was cloud-free enough to
81 allow a comprehensive post-classification interpolation. Based on our analysis of clouds
82 identified by Fmask algorithm, at least half of the available Landsat images acquired
83 between 2000 and 2020 presents missing observations over the coastal regions of Ghana.
84 There is a need for approaches that could comprehensively account for these gaps when
85 working with optical remote sensing data which are currently the best available source of
86 historical images in the coastal region of Ghana.

87 The use of continuous time series of satellite images, which provide consistently re-
88 peated observations of the earth's surface, can help improve the accuracy of mangroves
89 estimates in Ghana ([Lambin and Strahlers, 1994](#); [Verbesselt et al., 2010](#); [Zhu and Wood-](#)
90 [cock, 2014](#)). However, differences due to remote sensing artifacts in these multitemporal
91 images may cause error in comparative image analysis. Change detection analysis, there-
92 fore, should involve comparable data (i.e., similar sensors, similar radiometric and spatial
93 resolutions, similar viewing geometries, similar image anniversaries). The reliability of
94 comparative image analysis for change detection such as post-classification, temporal im-
95 age differencing, temporal image ratioing, depends on various environmental and atmo-
96 spheric factors and the accuracy of their resulting change detection analysis depends on
97 the accuracy of the input data. Error in the input images is likely to have compounding
98 effects in the change detection results. These approach, however, are intuitive, simple to
99 implement, and provide quantitative change estimates across a variety of LULC. Yet, for
100 these conventional methods to effectively support any operational application, data input
101 should be comparable across the spatial and temporal domains of the analysis ([Lillesand](#)
102 [et al., 2015](#)). Multitemporal image analysis should account for potential sources of un-
103 certainty such as imperfection of cloud masking algorithms, sensor differences, and other
104 ephemeral changes induced by erratic events that could introduce error in the classifi-
105 cations ([Zhu and Woodcock, 2014](#)). Multi-date images should be of the same period to
106 account for differences in sun angle and temporal variability in LULC. Post-classifications

for change detection should account for all major LULC while considering reference data (i.e., training and validation data) over areas of persistent LULC. Besides the requirements for training and validation for LULC classifications, it is important to ensure the comparability of the LULC classifications (Lillesand et al., 2015; Zhu and Woodcock, 2014). This can be achieved by either using a single classifier that is consistent with all classifications considered or ensuring that throughputs and accuracies are comparable when using multiple classifiers. These basics requirements have strong implications for the accuracy of change detection analysis that rely on multitemporal image classification. These requirements are often difficult to satisfy due to the lack of ideal satellite images. While Landsat collections are currently the best publicly available source of data that provide a reasonable and consistent synoptic estimate of land surface state within acceptable spatial resolution for studying changes in mangrove vegetation, it is virtually impossible to obtain the ideal pair of Landsat images in the coastal regions of Ghana. In these areas, the persistence of thick cloud layers reduces the number of usable images (Rubin et al., 1999). Consequently, these images are not always available at the nominal revisit period of 16 days for every pixel.

To address the issues mentioned above, we propose an approach that exploit the landscape phenology to reconstruct comparable data that account for the temporal behaviour of LULC. To ensure data comparability we masked out cloudy pixels and harmonized all available images across different Landsat sensors. To reconstruct gap-free continuous times series we used time-series statistical models to remove the noisy data, fill in missing data and recover the main signal. Based on this signal, we used unsupervised classification to identify areas of persistent LULC. To provide temporally consistent reference data for accurate multi-date classifications and change detection, we tailored our reference data to these persistent LULC. In doing so, the approach accounts for major sources of bias and limits the chance of propagating classification errors into change detection results. Our goal is to provide consistent up-to-date estimates of mangrove vegetation dynamics of Ghana based on continuous time series of remotely-sensed data acquired between 2000 and 2020. We used all available Tiers 1 and Tiers 2 Landsat data available in Google

¹³⁶ Earth Engine cloud computing platform to classify the existing LULC of Ghana into 17
¹³⁷ categories and study the dynamics of mangrove vegetation.

¹³⁸ **2. Study area and data**

¹³⁹ *2.1. Study area*

¹⁴⁰ Bordered by Côte d'Ivoire to the west, Burkina Faso to the north and Togo to the
¹⁴¹ east, Ghana is located on the West African shore of Atlantic Ocean. The country has a

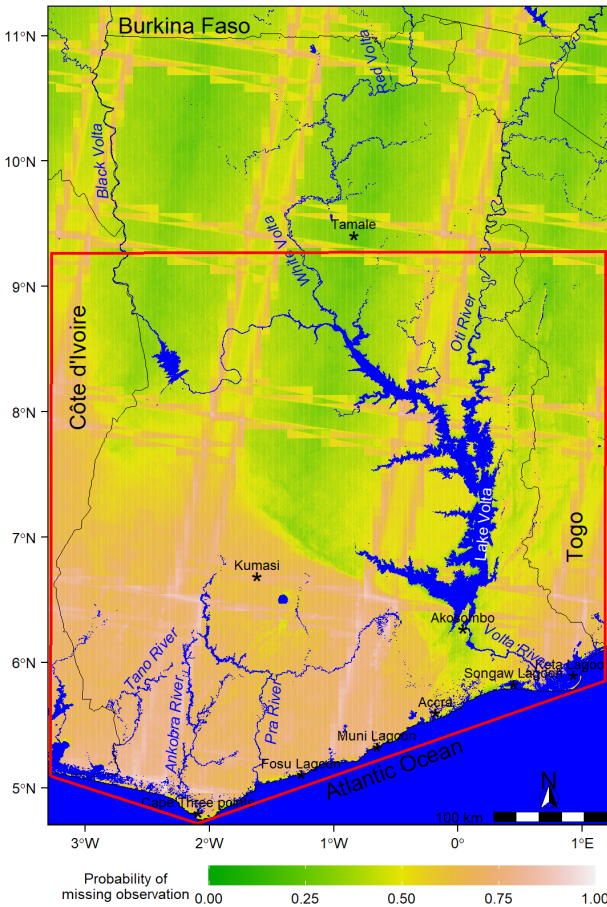


Figure 1: Major features and probability of missing data in Landsat collection between 1999 and 2020 in Ghana. The red box represents an area of interest and sampling frame for a spatial analysis of mangroves in Ghana. The probability of missing observation is estimated, as the ratio between the total number of missing data and the total number of acquisitions, based on all remote sensing artifacts as identified by Fmask algorithm.

¹⁴² rich body of fresh, and salty waters among which the major ones include the red Volta,
¹⁴³ the Black Volta and the White Volta rivers that originate in Burkina Faso to flow into
¹⁴⁴ Lake Volta and its estuary (Figure 1). Ghana has a coastline of about 550 km and over
¹⁴⁵ 100 estuaries and lagoons ([Levy et al., 2015](#)).

146 As of 2010, the population of Ghana is estimated at nearly 25 million, with an annual
147 population growth rate of 3.1 per annum ([Ghana Statistical Services, 2012](#)). The coastal
148 regions (e.g., Accra, Cape Coast) have the highest population density ([Addae and Oppelt,](#)
149 [2019](#)). These coastal regions experience two rainy seasons between March to July and
150 September to November, with an annual average temperature of about 26.8 °C. The
151 monthly temperature ranges from 24.7 °C in August to 33 °C in March. While Landsat
152 remained the publicly available source of data that provides the best compromise between
153 spatial and temporal resolutions in Ghana until Sentinel data become available in 2015,
154 the persistence of cloud poses an important problem for optical remote sensing application
155 ([Ashiagbor et al., 2021](#)). The chance of obtaining a clear observation at a given pixel rarely
156 exceed 0.5, particularly in the coastal region (Figure 1). This limits the amount of usable
157 data ([Ashiagbor et al., 2021](#)), making it difficult to map the entire landscape. This is a
158 region of intensive LULC changes due to anthropogenic activities. Most of these changes,
159 however, are gradual, meaning that the phenology of LULC remains more or less stable
160 over a relatively short period (e.g., 2 to 3 years). For pixels where remote sensing data
161 are available, this phenology can be easily described using time series statistical models.

162 In these areas, mangroves play important roles (e.g. habitat for various migratory birds
163 and fish species, fishing ground, timber for construction, wood fuel, herbal medicine,
164 spiritual places) for rural livelihood ([Armah et al., 2005; Spalding et al., 1997, 2010;](#)
165 [UNEP, 2007](#)). A decade ago, the total area of mangroves in Ghana ranged between
166 137 km² and 140 km² ([Armah et al., 2009; UNEP, 2007](#)). In Ghana, mangroves are
167 generally found around lagoons all over the coastline and Volta River Estuary (Figure
168 1). The most developed are found on the west coast (Côte d'Ivoire border to Cape
169 Three Points) ([Spalding et al., 1997](#)). Their distribution appears to follow the gradient of
170 salinity, with *Rhizophora* species encountered around open lagoons whereas species such
171 as *Avicennia germinans*, *Conocarpus erectus*, *Laguncularia racemosa* and *Acrostichum*
172 *aureum* are found around closed lagoons ([Spalding et al., 1997](#)). While mangroves play
173 key roles in the coastal regions of Ghana, existing studies of mangroves in Ghana appear
174 to generally concur with net declines in mangrove vegetation cover across the country.

175 Ghana has a reach body of LULC (e.g., water bodies, forests, savannas, shrublands,
 176 croplands), which are difficult to discriminate due to the important cloud cover, partic-
 177 ularly in the coastal regions (Figure 1). To accurately capture all mangroves vegetation
 178 and its dynamics, we considered all major LULC considering the whole country from East
 179 to West on a section spanning from the Atlantic Ocean to latitude 9.23 (Figure 1; red
 180 box). Our area of interest covers the Worldwide Reference System Path 192 to 196 and
 181 Row 053 to 057.

182 *2.2. Satellite imageries*

183 To consistently capture the phenology of LULC and provide accurate estimates of
 184 mangroves in Ghana, we considered all Landsat Tiers 1 and Tiers 2 collections, available

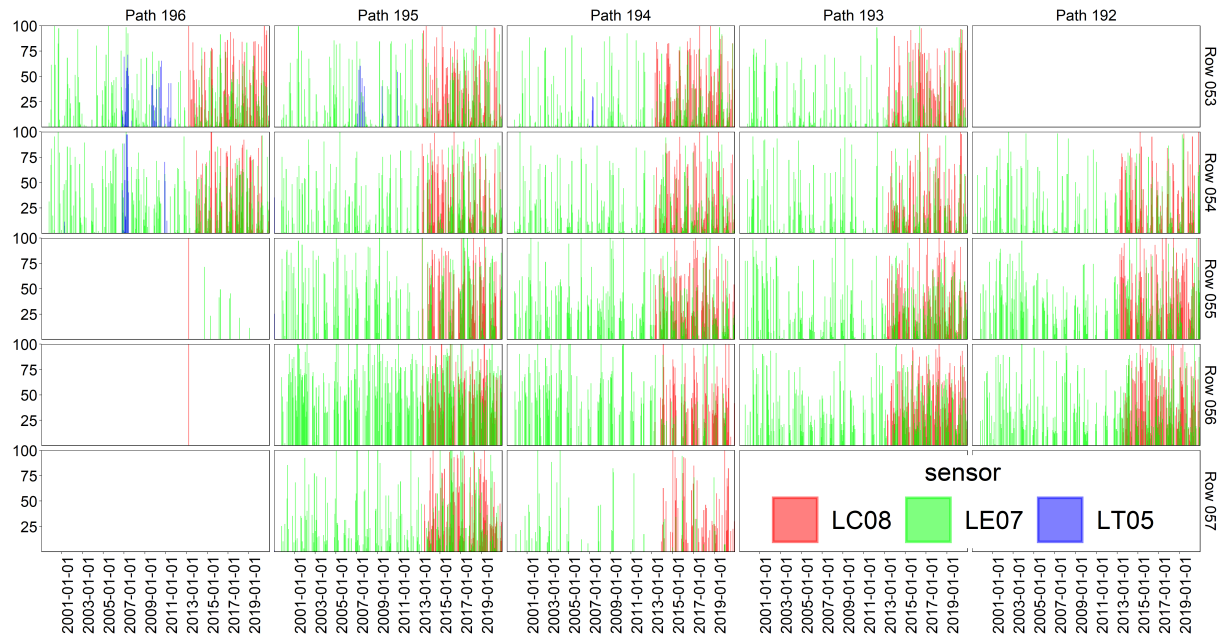


Figure 2: Percent cloud cover of Landsat collection in Ghana between 1999 and 2000. The acronyms in the legend represent the different Landsat sensors, with LC08 for Landsat 8 OLI - TIRS (Operational Land Imager and Thermal Infrared Sensor), LE07 for Landsat 7 Enhanced Thematic Mapper Plus and LT05 for Landsat 5 Thematic Mapper

185 from Google Earth Engine cloud computing platform ([Gorelick et al., 2017](#); [Wulder et al.,](#)
 186 [2019](#)), acquired between 1999 and 2020. We used a total number of 6409 Landsat tiles,
 187 each of which composed of 6 bands covering the 3 visible bands, the near infrared band,
 188 and the 2 short wave infrared bands. We considered the blue (0.45 - 0.52 μm), the green
 189 (0.52 - 0.60 μm), the red (0.63 - 0.69 μm), the near infrared or NIR (0.77 - 0.90 μm),
 190 the shortest wave infrared or SWIR1 (1.55 - 1.75 μm) and the longest wave infrared or

¹⁹¹ SWIR2 (2.09 - 2.35 μm) Landsat channels to account for different frequency ranges along
¹⁹² the electromagnetic spectrum in relation to differences in the reflectance of LULC. These
¹⁹³ atmospherically corrected data are suitable for LULC analysis since the surface reflectance
¹⁹⁴ values are comparable to those measured on the ground. They are also good candidates
¹⁹⁵ for change detection because they account for major atmospheric factors such as clouds,
¹⁹⁶ cloud shadow and aerosol scattering.

¹⁹⁷ Cloud and cloud shadow are the main factor limiting the amount of usable Landsat
¹⁹⁸ images in the study area (Figure 1; Figure 2). While cloud cover often reaches 100 % in
¹⁹⁹ most areas of Ghana, the coastal regions appear to be the cloudiest (Figure 1). Cloud
²⁰⁰ cover appears to persist throughout the year over the rows 055 and 056, with the path
²⁰¹ 195 being the most affected. We noted that nor Tiers 1 neither Tiers 2 data from Landsat
²⁰² 4 Thematic Mapper are available between 1999 and 2020 over Ghana. Only 85 images
²⁰³ were available from Landsat 5 Thematic Mapper over the area of interest. This gap in
²⁰⁴ Landsat data suggests that some gap filling may be required when considering continuous
²⁰⁵ time series of Landsat data in the region.

²⁰⁶ Prior to image classification, we removed all cloudy observations, harmonized the data
²⁰⁷ across sensors, mosaic the tiles based on monthly (30 days) median composites, removed
²⁰⁸ the noisy data, filled in the missing ones, and recover the main signal for each pixel
²⁰⁹ (see section 3.1) for more details) for details). We assume that LULC remain essentially
²¹⁰ unchanged over a relatively short period (e.g., 3 years) in the area of interest and consid-
²¹¹ ered 3 reference periods for image classification. These are the period 2000 – 2002, the
²¹² period 2010 – 2012, and the period 2018 – 2020. We will refer to these as 2000, 2010
²¹³ and 2020 and their respective classifications as 2000-classification, 2010-classification and
²¹⁴ 2020-classification.

²¹⁵ 2.3. Considerations for data inputs and image classification

²¹⁶ We conducted extensive field survey to identify 17 LULC classes based on which we
²¹⁷ systematically collected reference data for training and validation of LULC classifications.
²¹⁸ To provide a comprehensive LULC nomenclature, we defined most of these LULC classes
²¹⁹ (Table 1) based on the standard IGBP and FAO LULC classification systems ([Di Gregorio](#)

220 et al., 2016; FRA, 2000).

Table 1: Categories of land use and land cover used for an image classification in Ghana.

Standard class	Class description	Map legend
Water bodies	Natural and artificial Water bodies such as ocean, rivers, and other reservoirs containing fresh or salty water for the most period of the year.	Waters
Closed forests	Lands dominated by trees with a percent cover greater than 70 % during the entire period of the year.	Closed forests
Open forests	Lands dominated by trees with a percent cover between 60 and 70 % during the entire period of the year.	Open forests
Woody savannas	Lands with herbaceous and other understory systems, and with forest canopy cover between 30% and 60%. The forest cover height exceeds 2 m.	Woody savannas
Savannas	Lands with herbaceous and other understory systems, and with forest canopy cover between 10% and 30%. The forest cover height exceeds 2 m.	Savannas
Closed shrublands	Lands with woody vegetation less than 2 m tall and with shrub canopy cover > 60%. The shrub foliage can be either evergreen or deciduous.	Closed shrublands
Open shrublands	Lands with woody vegetation less than 2 m tall and with shrub canopy cover between 10% and 60%. The shrub foliage can be either evergreen or deciduous.	Open shrublands
Grasslands	Lands with herbaceous types of cover. Tree and shrub cover is less than 10%.	Grasslands
Permanent wetlands	Lands with a permanent mixture of fresh water and herbaceous or woody vegetation.	Wetlands
Croplands	Lands covered with temporary crops followed by harvest and a bare soil period (e.g., single and multiple cropping systems).	Croplands
Urban and built-up lands	Land covered by buildings and other man-made structures. This class includes all concrete cover, such as roads.	Built-up
Cropland and natural vegetation mosaics	Lands with a mosaic of croplands, forests, shrubland, and grasslands in which no one component comprises more than 60% of the landscape.	Mosaics
Barren	Lands with exposed soil, sand, rocks, or snow and never have more than 10% vegetated cover during any time of the year.	Barren
Mangroves	Lands with a permanent mixture of brackish water and herbaceous or woody vegetation.	Mangroves
Salt mines	Land with water of high salt concentration where the salt naturally emerges or is artificially extracted from evaporite formations.	Salt mines
Tree plantations	Land with perennial crop in the form of artificial forests. These are mostly represented by palm trees in the coastal region of Ghana.	Tree plantations
Regularly Flooded vegetation	Land transitioning between terrestrial and fresh water zones with sufficient moisture for the development of near evergreen vegetation.	Riparian vegetation

Note:

Regularly Flooded Vegetation, closed forests and open forests are based on FAO LULC classification system. Tree plantations are mostly represented by palm trees. The remaining classes are based on IGBP land cover classification system except for Mangroves which is the class of interest and Salt mines which is relevant in regards to mangroves vegetation dynamics in Ghana. Perennial woody crops are classified as either tree plantations (mostly palm trees) or the appropriate forest or shrub land cover type.

221 The first step in the collection of the reference data consisted of identifying regions
222 of dominant LULC and collecting large polygons over these regions. These reference
223 polygons are distributed over the area of interest in a way that captures the essential
224 LULC variability (both between and within class variability). The second step consisted
225 of identifying pixels of persistent LULC within each reference polygon and extracting the
226 reflectance values of these pixels from the multiband image. Pixels of persistent LULC
227 are pixels whose class remains unchanged across the reference periods considered. We
228 used these persistent pixels to ensure that the reflectance values used for training and
229 validation are consistent with the phenology of their corresponding LULC across the
230 reference periods.

231 The identification of the reference points involved the use of unsupervised classifica-
232 tions. For each reference period, we randomly sampled 1000 points and used k means
233 clustering algorithm to classify the image time series into 17 classes. We then identified
234 the LULC classes based on the reference polygons which also served as spatial bounding
235 boxes for sampling the reference points. We used stratified random sampling to extract
236 the reflectance values of the image time series over 700 reference points for each of the
237 17 classes. This required careful visual observation and matching of class configurations
238 across the entire landscapes of the classified images.

239 **3. Methods**

240 *3.1. Image pre-processing*

241 Prior to image classifications, we conducted a number of tasks to minimize the effects
242 of external factors on the resulting LULC classification. These image pre-processing tasks
243 involved several steps including the masking of cloudy pixels, the scaling of reflectance
244 values across the different Landsat sensors, the removal of noisy data, gap filling, and
245 the processing of the phenological signal. We used the quality assessment band provided
246 along with the surface reflectance product to mask all cloudy pixels. Despite the similarity
247 of Landsat sensors, data from different sensors present a slight difference which can be
248 relevant for analysis involving multiple sensors such as cross-sensor time series, temporal

249 image composite, or gap filling. Therefore, we scaled the reflectance to the value range of
 250 OLI sensor using the harmonisation coefficients provided by Roy et al. (2016).

$$p_t = \beta_0 + \beta_1 t + A \cos(2\pi\omega t + \varphi) + e_t \text{ (Non-linear form)}$$

$$= \beta_0 + \beta_1 t + \beta_2 \cos(2\pi\omega t) + \beta_3 \sin(2\pi\omega t) + e_t \text{ (Linearized form)}$$

Where,

- β_0 is the intercept (Starting point of p)
 - β_1 is the slope (How fast p changes with time)
 - t is the time indexed at t_0, t_1, \dots, t_N (Time since the epoch in radians)
 - A is the amplitude (The peak)
 - ω is the frequency of oscillation ($\omega = 1$ for a single cycle)
 - φ is a phase shift (Time at which p reaches its peak)
 - $\beta_1 t$ is then, the linear term (Inter-annual variability)
 - $A \cos(2\pi\omega t + \varphi)$ is then, the harmonic term (Main signal as sinusoidal waveform)
 - e_t is the random noise
 - p_t is the predicted pixel value at time t
 - β_2, β_3 are the harmonic coefficients (Intra-annual variability)
- (1)

With,

- $\beta_2 = A \cos(\varphi)$
- $\beta_3 = -A \sin(\varphi)$
- $A = (\beta_2^2 + \beta_3^2)^{1/2}$
- $\varphi = \tan^{-1}(\beta_3/\beta_2)$
- $A \cos(2\pi\omega t + \varphi) = \beta_2 \cos(2\pi\omega t) + \beta_3 \sin(2\pi\omega t)$

251 Despite the recent improvements and its widespread use, the Fmask algorithm used to
 252 derive the quality assessment band in Landsat surface reflectance product has its limita-
 253 tions in that the algorithm may not always detect cloudy pixels (Zhu et al., 2015; Zhu and

254 Woodcock, 2014). Therefore, we used equation (1) in a Robust Iteratively Reweighted
 255 Least Squares (RIRLS) framework to identify and removed such noisy data along with
 256 other outliers induced by erratic events (e.g., fire or flooding) following the procedure
 257 described in Zhu and Woodcock (2014). We used sine and cosine functions to specify
 258 non-linear models whose parameters depend on the temporal distribution of clear pixel
 259 values as determined by Fmask algorithm (equation (1)). Our approach consisted in es-
 260 timating the required parameters for models having a seasonality component to estimate
 261 land surface reflectance across the 6 Landsat bands. This was done only for pixels having
 262 a minimum number of 15 clear observations. We consider 2 rainy seasons (i.e., $\omega = 2$
 263 in equation (1)) to account for the inherent phenology of ecological systems in the study
 264 area (e.g., bimodal distribution of rainfall and vegetation).

$$p_{(green,t)} - \bar{p}_{(green,t)_{RIRLS}} > 0.04 \text{ OR } p_{(SWIR1,t)} - \bar{p}_{(SWIR1,t)_{RIRLS}} < -0.04$$

Where,

- t is the time indexed at t_0, t_1, \dots, t_N (Time since the epoch in radians)
- $p_{(green,t)}$ is the observed pixel value of the green band at time t
- $\bar{p}_{(green,t)_{RIRLS}}$ is the robust predicted pixel value of the green band at time t
- $p_{(SWIR1,t)}$ is the observed pixel value of the SWIR1 band at time t
- $\bar{p}_{(SWIR1,t)_{RIRLS}}$ is the robust predicted pixel value of the SWIR1 band at time t

With,

- The green band corresponding to band 3 (0.53 - 0.59 μm) of Landsat 8 OLI-TIRS or band 2 (0.52 - 0.60 μm) of Landsat 7 ETM+ and Landsat 5 TM.
- The SWIR1 band corresponding to band 6 (1.57 - 1.65 μm) of Landsat 8 OLI-TIRS or band 5 (1.55 - 1.75 μm) of Landsat 7 ETM+ and Landsat 5 TM.
- The robust predicted corresponding to the predicted pixel value using RIRLS

(2)

265 We first used the model to screen out and mask all noisy observations by comparing the

266 robust model estimates against the observed pixel values (Zhu and Woodcock, 2014). A
 267 pixel value is considered as noisy and masked at any time step, when either the difference
 268 between the observed and predicted pixel value of the green band is greater than 0.04 or
 269 the difference between the observed and predicted pixel value of the shortest wave infrared
 270 band is less than 0.04 (equation (2)).

$$p_{(x,t)missing} = \begin{cases} \bar{p}_{(x,t)RIRLS}, if \\ p_{(green,t)} - \bar{p}_{(green,t)RIRLS} \leq 0.04 \\ OR \\ p_{(SWIR1,t)} - \bar{p}_{(SWIR1,t)RIRLS} \geq -0.04 \\ missing, otherwise \end{cases}$$

Where,

- t is the time indexed at t_0, t_1, \dots, t_N (Time since the epoch in radians)
- $p_{(x,t)missing}$ is the missing pixel value of the band x at time t
- $p_{(green,t)}$ is the observed pixel value of the green band at time t
- $\bar{p}_{(green,t)RIRLS}$ is the robust predicted pixel value of the green band at time t
- $p_{(SWIR1,t)}$ is the observed pixel value of the SWIR1 band at time t
- $\bar{p}_{(SWIR1,t)RIRLS}$ is the robust predicted pixel value of the SWIR1 band at time t

With,

- The green band corresponding to band 3 (0.53 - 0.59 μm) of Landsat 8 OLI-TIRS or band 2 (0.52 - 0.60 μm) of Landsat 7 ETM+ and Landsat 5 TM.
- The SWIR1 band corresponding to band 6 (1.57 - 1.65 μm) of Landsat 8 OLI-TIRS or band 5 (1.55 - 1.75 μm) of Landsat 7 ETM+ and Landsat 5 TM.
- The robust predicted corresponding to the predicted pixel value using RIRLS

(3)

271 After identifying and removing the noisy observations, we used the robust model esti-

272 mates to replace all cloudy observations (equation (3)). Note that the noisy observations
273 are kept missing at this stage. To recover the phenological signal and remove all noises,
274 we used equation (1) to fit an Ordinary Least Squares (OLS) model to the gap-filled data
275 and extracted the resulting signal which we used as inputs for LULC classification.

276 *3.2. Land cover classification and accuracy assessment*

277 The pre-processing of the land surface reflectance data resulted in a collection of 267
278 multiband images where each band is a complete dataset of monthly signal describing pixel
279 phenology. From this large image collection, we extracted the time series corresponding
280 to each reference period to make up a new sub-collection of 36 images, each of which
281 composed of 6 bands. The sub-collections were then flattened into a single multiband
282 image of 216 bands for image classifications.

283 Accuracy assessment is an important component of LULC classification and any sub-
284 sequent analysis. The first component of the accuracy assessment consisted in estimating
285 the performance of the harmonic model using the root mean square error to illustrate
286 how well does the model fit the input data across different bands and LULC type. It is
287 easy to produce statistically accurate maps that do not reflect the real-world situation
288 due to inadequate validation samples (e.g., sample size and spatial distribution). To pro-
289 vide the best accuracy assessment possible of the LULC classification, we fairly evenly
290 distributed our validation data, cover most of the area of interest using a large sample,
291 compute statistical accuracy metrics using the traditional confusion matrix, and used
292 informal assessments using Google Earth imageries (<https://www.google.com/earth/>)
293 of high spatial and temporal resolution. Giving more priority to validation than train-
294 ing, the 11,900 reference points were split into 30% for training and 70% for validation.
295 To conduct the LULC classification, we used a random forest model with a maximum
296 number of 100 trees for each reference period (Breiman, 2001; Oshiro et al., 2012). The
297 three classifiers have the same specification and produce a similar statistical accuracy. To
298 ensure the best class separability and produce accurate results, we used these classifiers
299 to classify and validate the image times series corresponding to their respective reference
300 period.

301 *3.3. Change detection in land cover*

302 Although mangroves are the main focus, we estimated the acreage of LULC conver-
303 sion across all the LULC classes involved in the classifications. We compared the 2000-
304 classification with the 2010-classification, the 2010-classification with the 2020-classifcation,
305 and the 2000-classification with the 2020-classifcation to identify class changes and com-
306 pute the total areas of LULC change between these reference periods in the area of interest.
307 We then examined the changes specifically involving mangrove vegetation. We screened
308 the LULC classifications of the 3 reference periods to identify all areas classified at least
309 once as mangroves to generate a mangrove mask which we used to mask all non-mangrove
310 pixels in the 3 classifications. Based on the resulting masked classifications, we estimated
311 the dynamics of mangroves as decrease, stability, and increase in mangrove areas. Areas
312 of decrease are areas where mangroves vegetation were replaced with other LULC as op-
313 posed to areas of increase, whereas areas of stability are areas where mangrove vegetation
314 persists.

315 **4. Results**

316 *4.1. Evaluation of model performance*

317 The harmonic model appears to have generally captured the phenology of the LULC
318 across all the 6 Landsat bands with the majority of pixels predicted with RMSE in the
319 range of 300 (Figure 3). Relatively high RMSE are rare. The model appears to have
320 achieved the best performance over the short-wave infrared channels with the shortest
321 wave infrared being the best predicted. The model performance over the shortest wave
322 infrared appears to be comparable to that over the near infrared. The model appears to
323 have achieved, more or less similarly, the lowest performance over the visible bands where
324 difference across tiles becomes more perceptible. In general, the model performance is
325 relatively poor over the coastal regions and areas of dense vegetation. While water bodies
326 appear to be essentially associated with the lowest RMSE, this RMSE appears to slightly
327 increase over riparian vegetation. In general, the performance of the model appears to
328 increase with wavelength and seasonality.

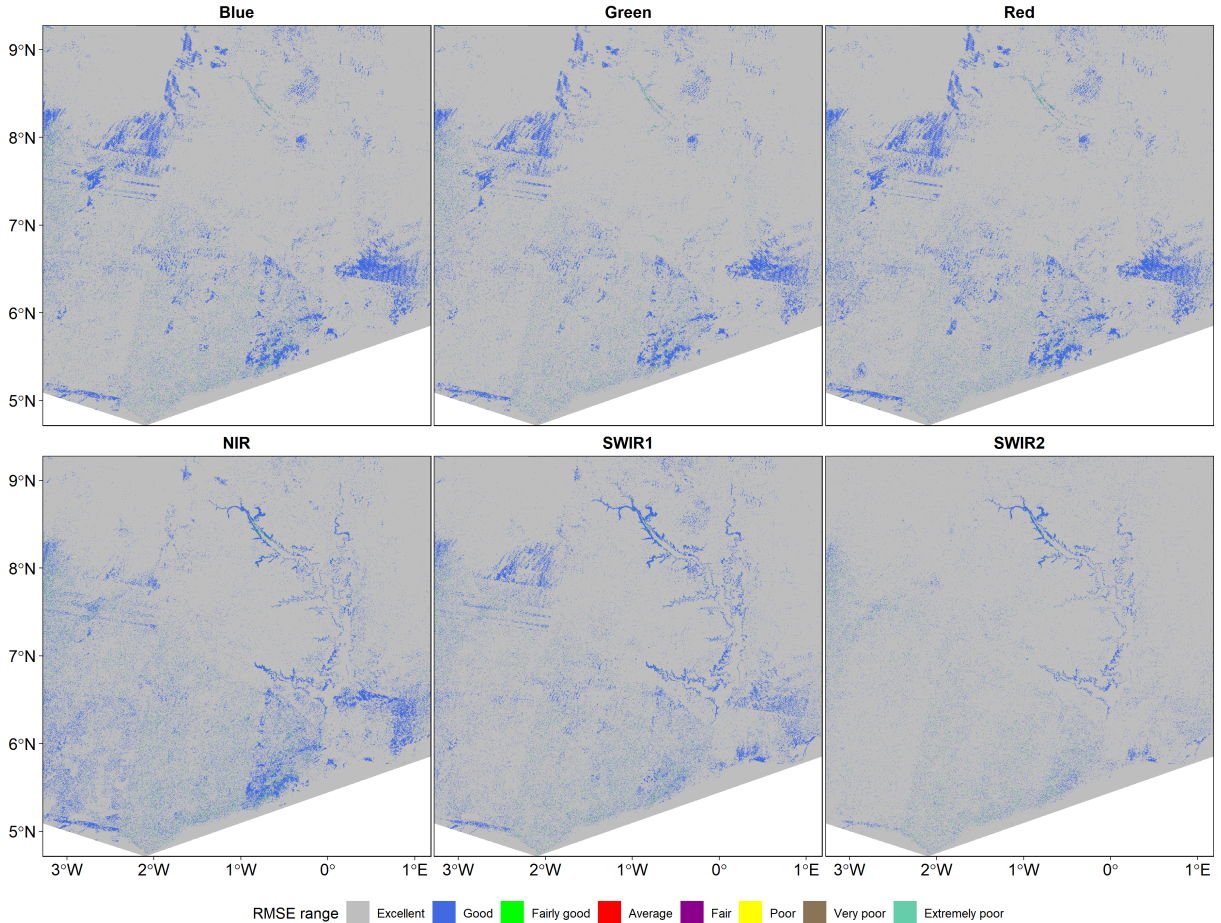


Figure 3: Prediction error of a spatially explicit harmonic model fit to 6 bands of Landsat surface reflectance over Ghana. The prediction error is estimated as root mean square error (RMSE). The RMSE was grouped to improve visualisation based on [Jiang \(2013\)](#)'s head / tail breaks as implemented in classInt R package ([Bivand, 2020](#)). The input data are in the range of thousands with the Likert scale in the legend corresponding to model performance and translating into the following RMSE range: Excellent = [0, 388[, Good = [388, 2990[, Fairly good = [2990, 48600[, Average = [48600, 584000[, Fair = [584000, 5200000[, Poor = [5200000, 38200000[, Very poor = [38200000, 136000000[, Extremely poor = [136000000, 389000000[.

The model performed generally well across the 17 LULC (Figure 4). The model achieved the best performance over LULC of medium vegetation density (i.e., savannas, shrublands and croplands). Relatively densely vegetated LULC (i.e., forests, tree plantation and riparian vegetation) and water bodies exhibit a slightly lower model performance. The lowest model performance is associated with non-vegetated LULC (i.e., barren, built-up) and marine LULC (i.e., mangroves and salt mines).

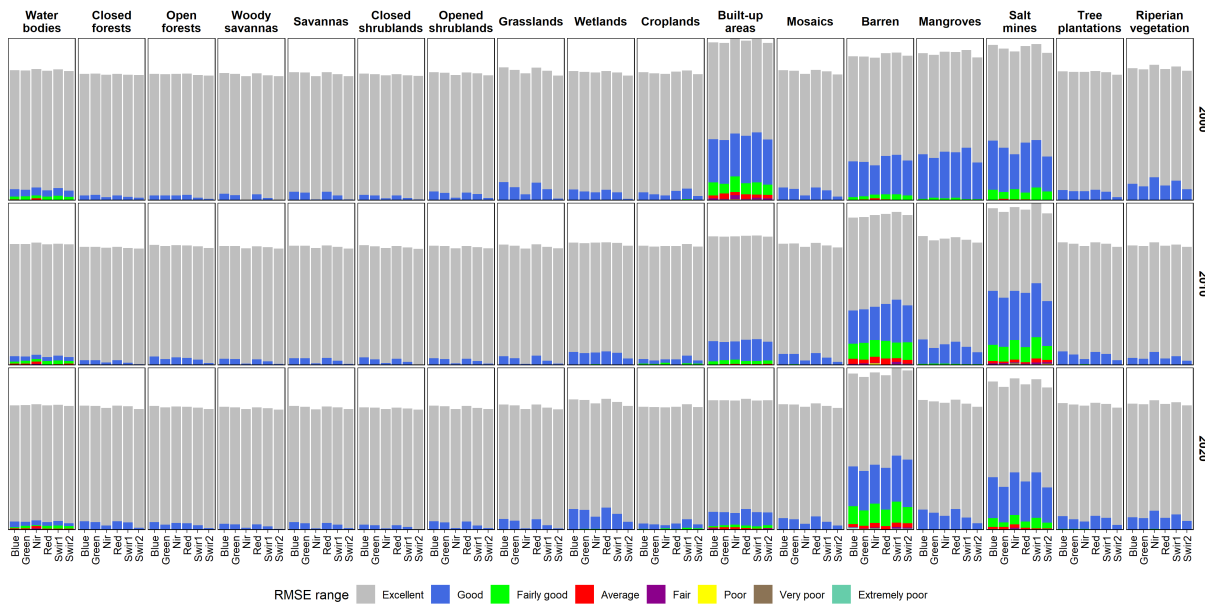


Figure 4: Prediction error of a spatially explicit harmonic model across different land use and land cover in Ghana. The prediction error is estimated as root mean square error (RMSE). The RMSE was grouped to improve visualisation based on [Jiang \(2013\)](#)'s head / tail breaks as implemented in classInt R package ([Bivand, 2020](#)). The input data are in the range of thousands with the Likert scale in the legend corresponding to model performance and translating into the following RMSE range: Excellent = [11.88, 681.24[, Good = [681.24, 7480.90[, Fairly good = [7480.90, 66315.81[, Average = [48600, 354635.13[, Fair = [354635.13, 1253545.74[, Poor = [1253545.74, 2548527.97[, Very poor = [2548527.97, 4229437[.

The results of the statistical accuracy assessment conducted using the confusion matrix approach show a minimum overall classification accuracy of 94% for 2020-classification and 2010-Classification, and a maximum of 95% for 2000-Classification. Kappa statistics range between 0.94 for 2020-classification to 0.95 for 2000-Classification (Table 2). The accuracy for individual LULC classes ranges between 80% and 100% for producer accuracy. These correspond to a minimum of 81% and a maximum of 100% for consumer accuracy. The mangrove class was detected with a producer accuracy ranging between 97% and 98%, and a consumer accuracy ranging between 91% and 97%.

Considering the number of classes (17 LULC classes), the even distribution of the val-

Table 2: Statistical accuracy assessment of multitemporal land use and land cover classifications of southern Ghana conducted for mangrove vegetation analysis. The input data were pre-processed using time series statistical models via harmonic modelling of all available Tiers 1 and Tiers 2 Landsat surface reflectance data acquired between 2000 and 2020. This accuracy assessment is based on random forest classifiers with a maximum number of 100 trees.

Land use and land cover class	2020-Classification		2010-Classification		2000-Classification	
	Consumers accuracy	Producer accuracy	Consumers accuracy	Producer accuracy	Consumers accuracy	Producer accuracy
Water bodies	0.99	1.00	1.00	0.99	0.99	0.98
Closed forests	0.88	0.80	0.99	0.96	0.96	0.92
Open forests	0.98	0.99	0.91	0.91	0.97	0.96
Woody savannas	0.84	0.83	0.92	0.90	0.96	0.92
Savannas	0.96	0.97	0.82	0.85	0.96	0.99
Closed shrublands	0.99	0.96	0.85	0.82	0.94	0.92
Opened shrublands	0.99	0.99	1.00	0.99	0.98	0.99
Grasslands	0.98	0.98	1.00	0.99	0.98	0.96
Wetlands	0.81	0.84	0.89	0.91	0.88	0.93
Croplands	0.93	0.99	0.91	0.99	0.90	0.97
Built-up areas	0.93	0.90	0.94	0.88	0.92	0.85
Mosaics	0.98	0.99	0.98	1.00	0.95	0.93
Barren	0.94	0.91	0.95	0.93	0.95	0.95
Mangroves	0.96	0.97	0.97	0.98	0.91	0.98
Salt mines	0.99	0.99	0.99	1.00	0.99	1.00
Tree plantations	0.84	0.89	0.90	0.92	0.98	0.98
Riperian vegetation	0.97	0.99	0.99	1.00	0.99	0.96
Overall accuracy	0.94		0.94		0.95	
Kappa	0.94		0.94		0.95	

344 validation points, and the number of 500 validation samples per class (8500 points in total),
 345 the results are satisfactory. These are consistent with the informal accuracy assessment
 346 conducted using the images from Google Earth. The classification appears to accurately
 347 represent the configuration of LULC classes on the ground. In some areas, however, it
 348 was not possible to track back these LULC through time due to the lack of temporal
 349 Google Earth imagery.

350 4.2. Land cover changes

351 At glance, major features in the coastal regions of Ghana are the closed forests en-
 352 countered between 3°W to 0°W and 5°N to 7°N, the water bodies including the network
 353 of Volta water bodies, the Atlantic Ocean, the built-up areas with major cities such as
 354 Accra and Kumasi being more visible, the tree plantations in the 2000-Classification, and
 355 the open forests in both the 2010-Classification and the 2020-Classification (Figure 5).

356 It appears from the LULC maps that closed forests have decreased over time. This
 357 forest degradation, particularly noticeable over the portion between 3°W to 2°W longitude

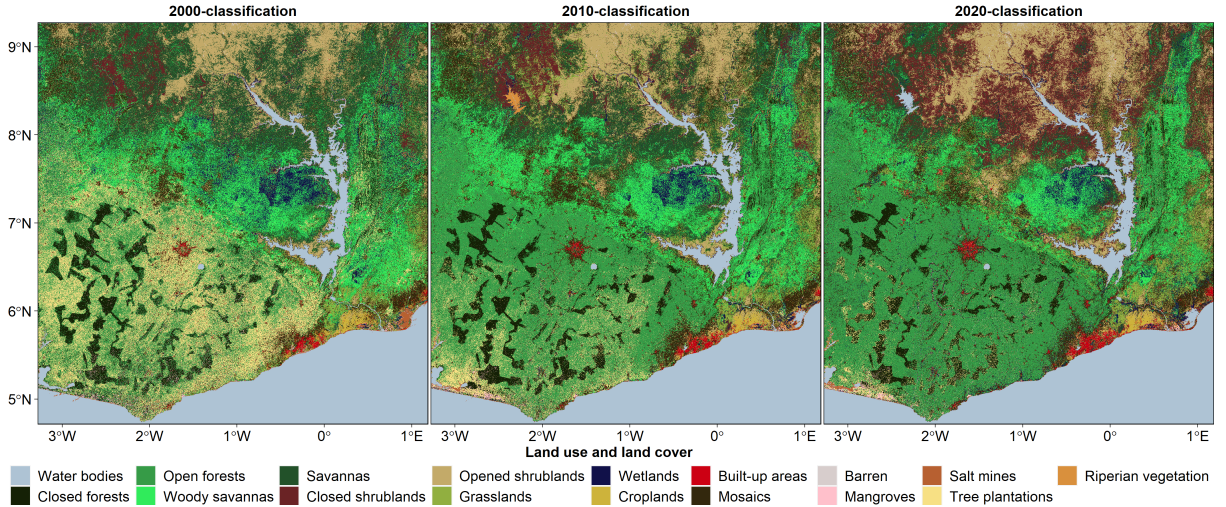


Figure 5: Multitemporal land use and land cover classifications of southern Ghana conducted for mangrove vegetation analysis. The input data were pre-processed using time series statistical models via harmonic modelling of all available Tiers 1 and Tiers 2 Landsat surface reflectance data acquired between 2000 and 2020. These classifications were based on random forest classifiers with a maximum number of 100 trees.

and 5°N to 6°N latitude, appears to be higher upon the period 2010 to 2020 than during the previous decade. Water bodies appear to have remained more or less stable, except for the appearance of some artificial reservoirs such as the Bui dam on the course of Black Volta towards the north. In the far most East towards the border with Togo, some salt mines appear to have become water bodies suggesting a possible sea level rise in this region. Built-up areas appear to have been increasing since 2000, suggesting an increased urbanization in the region. Mangroves appear to be visible only in the West Coast around the border with Côte d'Ivoire where they seem to have developed after the year 2000 since they are less visible at glance in this region on the 2000-Classification. In Ghana, mangroves are generally of small size and scattered along the coastline of the Atlantic Ocean.

Insights from image statistics revealed greater information than those visible at glance (Table 3). There is a slight increase in areas covered by water over the study period (2000 - 2020) which seems to have mostly occurred upon the period 2010 to 2020. Closed forest area has also slightly decreased even though this forest degradation appears to progressively hold upon the study period. The area covered by the open type of forests, in turn, has increased at a high rate over the study period. This increase appears to have occurred at the expense of closed forests with a similar rate over both study periods.

Table 3: Dynamics of major land use and land cover between 2000 and 2020 in Ghana. Data are reported in hectares of land. Change (2000 - 2020) is estimated by subtracting the 2020 estimates from the 2000 estimates. These changes are interpreted as slight (below 500,000 ha in absolute terms), moderate (between 500,000 and 1,000,000 ha in absolute terms), and high (above 1,000,000 ha in absolute terms).

Land use and land cover class	2020	2010	2000	Change (2000-2020)
Water bodies	634,865.30	593,369.60	593,782.60	41,082.70
Closed forests	993,152.80	1,085,267.90	1,148,749.00	-155,596.20
Open forests	4,940,904.00	4,440,366.00	2,854,193.00	2,086,711.00
Woody savannas	1,460,843.00	2,112,157.00	2,188,337.00	-727,494.00
Savannas	1,439,506.00	2,386,865.00	2,997,046.00	-1,557,540.00
Closed shrublands	2,124,826.10	866,632.00	529,264.90	1,595,561.20
Opened shrublands	1,986,620.00	1,722,579.00	1,516,987.00	469,633.00
Grasslands	769,840.20	861,989.00	360,629.30	409,210.90
Wetlands	797,702.80	536,080.60	836,869.00	-39,166.20
Croplands	97,584.86	85,591.05	101,394.68	-3,809.82
Built-up areas	171,858.60	112,050.20	117,516.60	54,342.00
Mosaics	1,475,992.00	1,612,346.00	1,172,785.00	303,207.00
Barren	74,014.78	20,345.02	20,845.76	53,169.02
Mangroves	52,691.18	46,587.36	121,475.94	-68,784.76
Salt mines	28,082.26	31,541.75	50,014.97	-21,932.71
Tree plantations	278,965.10	780,588.20	2,720,081.50	-2,441,116.40
Riperian vegetation	93,552.30	126,645.15	91,028.86	2,523.44
Total	17,421,001.28	17,421,000.83	17,421,001.11	

376 Savanna lands have experienced a high decrease with woody savannas being less affected
 377 than savannas. While the decrease in woody savannas area appears to have essentially
 378 occurred upon the period 2010 to 2020, the decrease in savannas area appears to have
 379 been happening upon the entire study period at an increasing rate. Shrubs, in contrast
 380 to savannas, have been gaining land areas since the year 2000. Closed shrublands, which
 381 show a higher increase rate than open ones, have experienced a high increase while the
 382 increase in open shrublands has been moderate. Cropland area appears to be stable,
 383 meaning that changes in agricultural lands are fundamentally attributed to cropland and
 384 natural vegetation mosaics which have seen a slight increase upon the period 2000 to
 385 2010. The area covered by tree plantations appears to have highly decreased, particularly
 386 between the years 2000 and 2010. Overall, mangrove vegetation area has experienced a
 387 slight decrease upon the overall study period. This mangrove degradation appears to have
 388 essentially occurred upon the period 2000 to 2010. However, mangrove coverage seems
 389 to have increased over the period 2010 to 2020, even though at a lower rate compared to
 390 the previous decade.

Table 4: Mangrove vegetation dynamics in relation to other land use and land cover between 2000 and 2020 in Ghana. Data are reported in hectares of land for both gains and losses. These gains and losses are interpreted as slight (below 5,000 ha), moderate (5,000 - 10,000 ha), and high (above 10,000 ha).

Land use and land cover class	2000 - 2010		2010 - 2020		2000 - 2020	
	Gain	Loss	Gain	Loss	Gain	Loss
Water bodies	1,970.69	665.27	230.68	498.24	1,123.99	1,941.08
Closed forests	10,405.53	42,027.66	9,959.94	7,970.94	12,541.06	31,145.81
Open forests	4,245.51	24,445.83	2,070.32	3,556.10	7,395.80	37,435.64
Woody savannas	9.79	738.95	38.22	87.54	234.43	1,472.81
Savannas	11.74	257.18	43.20	19.75	147.05	546.29
Closed shrublands	23.96	182.41	5.69	8.98	42.81	416.11
Opened shrublands	7.90	255.83	34.96	41.17	95.57	1,127.07
Grasslands	11.42	361.62	32.55	7.47	302.02	506.06
Wetlands	1,448.30	4,211.22	2,613.68	922.08	2,563.10	5,602.48
Croplands	0.71	4.36	18.51	3.65	45.63	92.20
Built-up areas	29.53	346.73	50.15	98.79	340.14	1,274.09
Mosaics	46.19	1,780.36	267.37	336.17	1,002.19	7,111.21
Barren	5.60	82.22	23.04	92.88	55.66	1,656.30
Salt mines	1,521.19	1,711.93	357.76	642.00	438.68	2,104.20
Tree plantations	722.18	15,141.73	7,991.87	6,617.72	6,235.15	9,291.56
Riperian vegetation	2,383.93	5,519.47	4,139.16	869.84	3,979.60	3,604.72
Total	22,844.19	97,732.77	27,877.13	21,773.31	36,542.88	105,327.64

4.3. Mangrove vegetation dynamics

The overall assessment of mangrove areas dynamics shows that mangrove vegetation

experienced different trends in Ghana, with areas of improvements and declines (Table

4). Examining the source of mangrove areas dynamics, our results show that forests,

wetlands, cropland and natural vegetation mosaics, and tree plantations are the top most

important causes of mangrove losses. Mangroves have experienced high gains at the

expense of closed forests and moderate gains at the expense of open forests, but neither

the gain at the expense of closed forests nor the gain at the expense of open forests has

compensated for the equivalent losses over the study period. Mangroves experienced high

losses in favour of closed forests and open forests. We observed moderate losses in favour

of cropland and natural vegetation mosaics and tree plantations. While mangrove gains

at the expense of tree plantations compensated for the corresponding losses, mangrove

gains in relation to cropland and natural vegetation mosaics are much lower than the

corresponding losses. Even though in the range of minor loss, substantial acreage of

mangrove became barren, of which only less than a tenth was recovered over the study

period.

407 *4.4. Site-specific analysis and mangrove change direction*

408 The findings of the LULC analysis provide useful insights into the overall dynamics
409 of LULC in the coastal regions of Ghana. In this section, we attempt to provide further
410 information for operational application in mangrove conservation by identifying areas of
411 mangrove increase and decline in a spatially explicit manner. Herein, we present the
412 major mangrove areas of Ghana in some sort-of case studies for conciseness and better
413 visualisation. For a complete picture of mangrove dynamic in Ghana, we refer the reader
414 to the technical materials (see Software and data availability). We presented 10 different
415 cases covering most of the major mangrove areas of Ghana. These include urban mangrove
416 vegetation, those found around rivers, and those found around lagoons. Despite the
417 declining trend observed over the past decade, many of these areas appear to generally
418 exhibit a stable trend during the last decade.

419 Mangrove coverage in the West Coast of Ghana appear to have remained dominantly
420 stable over the study period, particularly during the period 2010 to 2020 (Figure 6).
421 Major spots of this stability are found around the trench between Tikobo 1 and Aiyinase
422 through Amansuri Lake. This area has seen important mangrove expansion before 2010,
423 period after which the area seems to have dominantly stabilised. While most of the area
424 exhibits a stable trend, several spots show a declining trend in mangrove vegetation cover
425 suggesting that the area tends towards a decline. Beyond Tikobo 2 to the north, however,
426 only small patches of mangroves remain before 2000, period after which these mangroves
427 were converted into other LULCs. Other spots of mangrove degradation are found around
428 Half Assini where most mangroves seem to have disappeared over the last decade. Slightly
429 to the south of Half Assini, mangrove coverage appears to have substantially increased
430 over the study period.

431 In the vicinity of Kpani river, mangrove coverage essentially remained stable over the
432 study period, with localised spots of decrease and increase (Figure 6). In the Kpani River
433 basin, localised spots of mangrove area expansion are encountered in southeast of Miemia
434 along the left branch of Kpani River as well as in the north of Lake Ehunli Lagoon along
435 the right branch of the Kpani River. The regeneration near Miemia seems to have essen-

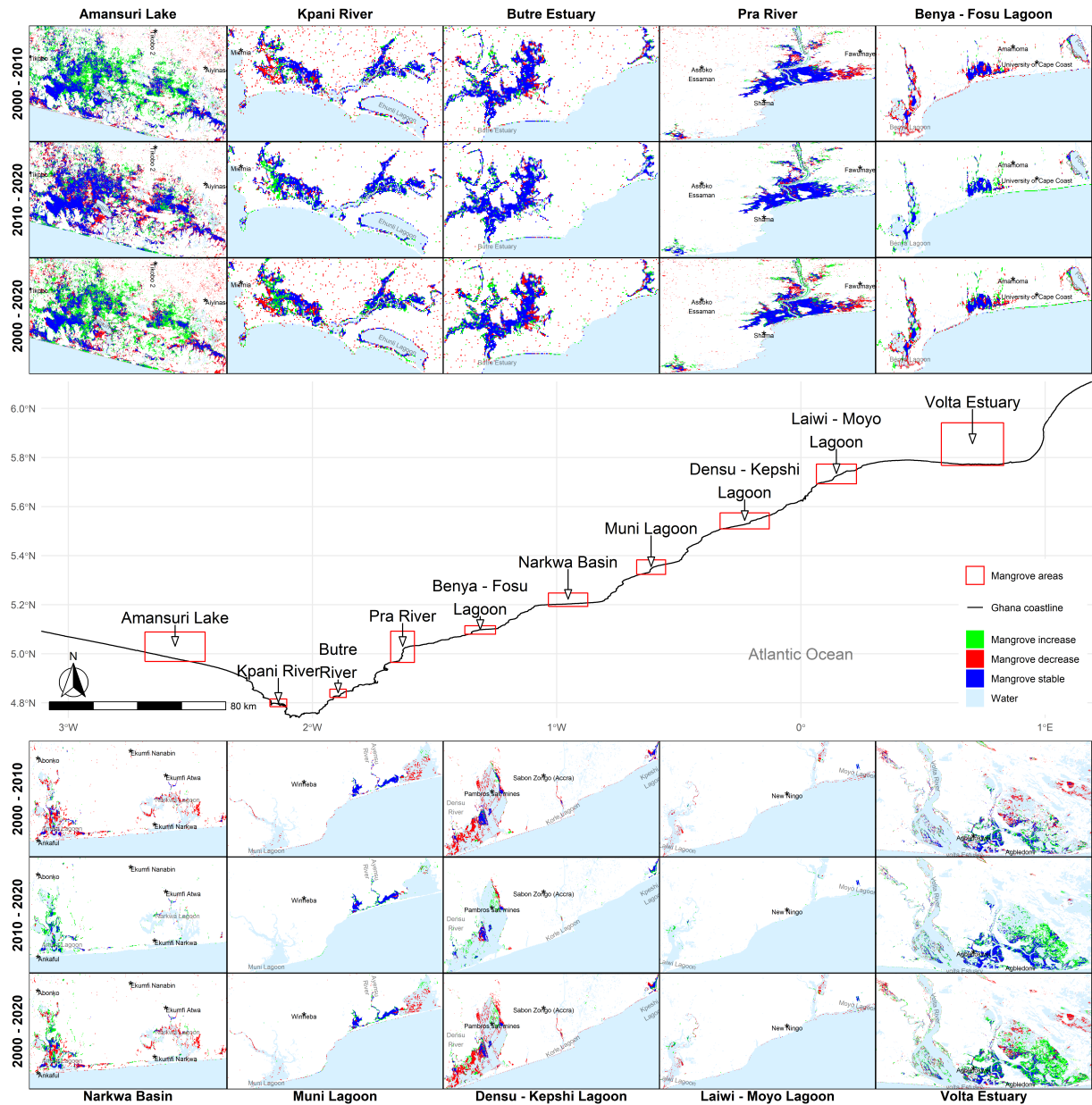


Figure 6: Dynamics of mangrove vegetation in selected mangrove areas of Ghana.

tially taken place during the period 2010 to 2020. Minor mangrove coverage expansion
is observed in the southern shore of Ehunli Lagoon, but the mangrove area around the
lagoon seems to be in decline over the study period. Beyond the proximity of Kpani River
and Lake Ehunli Lagoon, the mangrove area appears to have been substantially declining
long before 2000, leaving only a few patches scattered all over the region. These mangrove
remains seem to have mostly been converted into other LULCs after 2010. Kpani River
presents a similar trend of stability compared to Ezile River near Akwidaa (not presented
here). However, in Ezile River, the regeneration appears to be negligible compared to the
degradation affecting most of the landmass between Akwidaa and Dixcove. In this area
where little has been gained, the stability of the mangrove area is limited to the riverbank,
beyond which mangroves are essentially in decline over the study period.

Along Butre River and its upper tributaries on either side of the river, mangroves
appear to have regenerated between 2000 and 2010. In the lower tributary giving rise
to the eastern floodplain, mangroves appear to have predominantly decreased at the
periphery of the floodplain which represent the hotspot of Butre River mangroves. Both
areas of gain and loss appear to have kept the same trend between 2010 and 2020, even
though at a lower rate compared to previous decade. Further to the East of Butre River
in Takoradi town, mangroves appear to have substantially declined over the study period
(Figure 6), despite the few stable mangrove spots around water bodies. Except for the few
spots of stability around water bodies, mangroves in Takoradi town of Ghana appear to
have substantially declined over the study period (Figure 6). Mangrove area in this region
seems to have declined even before 2000. Close to the water bodies, we noticed both areas
of stability, decline and increase, but mangrove area increase and decline appears to be
only limited to the immediate proximity of these urban water ways. These remaining
mangrove areas, however, seem to remain stable with a few regeneration patches over the
period 2010 and 2020.

For the most, mangrove area around Pra River kept a stable trend over the study
period (Figure 6). Mangrove area has remained dominantly stable on either side of Pra
river, particularly in the immediate proximity of the Atlantic Ocean. Mangrove area seems

465 to have increased in some areas close to the Atlantic Ocean directly below Fawumaye.
466 This regeneration gradient appears to circumvent Fawumaye following an arc reaching
467 up to the northern part of the town. Beyond this point, only few patches of mangroves
468 remain before 2000, period after which they have mostly disappeared. The same situation
469 is observed around Assako Essaman. Another spot of regeneration is observed directly
470 below Assako Essaman on the shore of Atlantic Ocean. In this relatively small area,
471 mangrove area appears to have increased during the last decade, essentially compensating
472 for the lost they have seen over the period 2000 to 2010.

473 In Cape Coast town of Ghana, mangrove area shows a stable trend with many spots of
474 increase, suggesting that mangrove vegetation have seen an interesting regeneration over
475 the study period (Figure 6). While our results are not conclusive regarding the situation
476 of mangrove vegetation in the town before 2000, the consistent declining trend observed
477 over all mangrove areas along with the few spots of decline across the town during the last
478 decade suggest that some mangrove areas were converted into settlement long before 2000.
479 This is supported by the declining trend near Amamoma where mangroves appear to have
480 undergone important degradation following the ongoing urban expansion in Amamoma
481 belt of Cape Coast.

482 This settlement encroachment appears to have started long before 2010. The mangrove
483 area appears to have considerably shrunk over the last decade, suggesting that these
484 mangroves are likely to disappear in the near future. Other spots of mangrove decline in
485 Cape Coast town of Ghana are found around Fosu Lagoon where most of the surrounding
486 mangroves have been converted over the study period. However, the overall mangrove area
487 appears to have increased over the last decade in Cape Coast. Except for Fosu Lagoon,
488 stable to increasing trend appears to prevail in most mangrove sites over the period 2010 to
489 2020. Upon this period, the remaining mangroves near Amamoma remained dominantly
490 stable while those in Benya Lagoon were inclined towards an increasing trend.

491 Mangroves in Narkwa region have experienced important decline during the period
492 2000 to 2010 (Figure 6). Except for a few spots showing stable to increasing trend
493 in Amisa Lagoon, almost all mangrove in the region were depleted during this period,

494 particularly in Narkwa Lagoon. However, substantial mangrove areas have recovered over
495 the last decade. Along the land mass spanning from Anboko to the eastern parts of the
496 twin Ekumfi through Ankaful, only a few spots of decline are observed in 2020. This mean
497 that mangroves in the region have essentially recovered from the important degradation
498 that took place during the previous decade. Overall, the region appears to have gained
499 appreciable mangrove coverage in Amisa Lagoon near Ankaful as opposed to Narkwa
500 Lagoon showing a leading trend of mangrove degradation.

501 The dynamics of mangrove area in Muni Lagoon is dominated by an increasing trend
502 over the study period (Figure 6). This area appears to be deprived of mangroves vegeta-
503 tion before 2010. The few spots of mangrove degradation around the lagoon and along the
504 coastline in the East of the lagoon during the period 2000 to 2010 suggest that mangroves
505 have experienced an unprecedent decline before 2000. The current mangrove vegetation
506 in the lagoon dates back to no more than 2010 since no mangroves were observed before
507 2010 in the lagoon.

508 Like in Muni Lagoon, an increasing trend dominated the neighbouring Ayensu River.
509 In this area, however, mangroves vegetation dates back to 2000, meaning that some
510 mangrove areas remained stable over the study period. Beyond the lower tributary of
511 Ayensu River to the East, however, substantial mangrove areas appear to have emerged
512 at the expanse of salt mines. This area has seen important mangrove regeneration over
513 the last decade.

514 In Accra town of Ghana, mangrove area appears to have increased over the study
515 period (Figure 6). Most mangrove areas between Densu and Kepsi Lagoon appear to
516 exhibit stable trends, with the majority of them inclined towards an increase. Mangrove
517 area gains are observed all over Densu region (Densu River and Densu Estuary including
518 Densu Salt Mines). These mangrove area gains appear to have taken place in the west-
519 ern part to consistently progress northwards. In this area where we observe important
520 mangrove regeneration, mangroves appear to have gained substantial land areas at the
521 expanse of salt mines. Except for a few spots of declines, mangrove area appears to have
522 increased over the banks of Densu River.

523 In Densu region, area of mangrove loss appears to be limited to Densu Estuary, par-
524 ticularly at the periphery of Densu Salt Mines where substantial losses in favour of set-
525 tlements are observed from nearly Mallam Mosque up to the upper border of Densu Salt
526 Mines. The lower part of the estuary (between the lower border of Densu Salt Mines and
527 the shore of Atlantic Ocean) shows a mixture of stable, increasing and declining man-
528 grove areas over the study period. Despite a few spots of decline, mangrove area appears
529 to have increased over the study period in Korle Lagoon. Mangrove area has shrunk in
530 favour of settlements in the left branch of Kpeshi Lagoon whereas this area has essentially
531 expanded over the right branch and the lower part of the lagoon.

532 In Accra, mangrove area appears to have seen important decrease over the decade
533 2000 to 2010 with major mangrove areas, including Densu estuary, Korle Lagoon and
534 Kpeshi Lagoon, exhibiting a stable to declining trend of mangrove vegetation. Only a
535 few spots of mangrove area increase, essentially in Densu Estuary and Kpeshi Lagoon
536 are observed between 2000 and 2010. It appears that most of the mangrove vegetation
537 in Densu River has emerged after this period. Except for relatively minor loss due to
538 urbanisation that appears to continuously encroach on mangrove area, mangrove vegeta-
539 tion has widely spread over the last decade, resulting in Densu region and Korle Lagoon
540 exhibiting increasing trends, and Kpeshi Lagoon showing stable to increasing trend in
541 mangrove area.

542 The land portion between Laiwi and Moyio lagoons of Ghana is a dominantly an
543 agriculture region where croplands extend to the coastline of Atlantic Ocean. In this
544 region, mangrove vegetation appears to be tightly limited to the immediate proximity
545 of lagoons and coastline (Figure 6). Mangrove vegetation appears to have increased
546 everywhere around lagoons and along the coastline between Laiwi and Moyo lagoons over
547 the study period. Except for relatively minor losses scattered over the region, we only
548 noted a few spots of stable mangrove vegetation mostly over abandoned salt mining areas.

549 Given the presence of a few scattered tickets of mangrove vegetation before 2000 and
550 the absence of these in 2010, we presume that mangrove vegetation in the region was
551 depleted before 2010. Essentially, these mangroves appear to have regenerated during the

552 last decade.

553 The Eastern Coasts of Ghana show both increasing and stable trends in mangrove
554 area, along with areas of stable mangrove vegetation over the study period. In general,
555 however, mangrove area appears to have increased in the western part of the region.
556 Spots of decreasing mangrove areas, which appear to augment northwards, are mostly
557 encountered in the central part of the region. In the western part, mangrove area appears
558 to have increase around Lake Songaw Lagoon where we only observe a few declining
559 spots at the periphery of the lagoon. In the central part, mangrove area appears to
560 have decreased in volta River and the western part of Volta Estuary. In this part, we
561 only observe a few stable to increasing trend of mangrove vegetation towards the shore
562 of Atlantic Ocean. Mangrove vegetation in the eastern part of Volta Estuary, where we
563 observe consistent mangrove stability over a large area between the estuary and Keta
564 Lagoon, appears to have remained stable or increased over the study period. Relatively
565 fewer mangroves are observed towards the Togolese border around Keta Lagoon where
566 most of these appear to show an increasing trend with a few spots of decline.

567 Mangrove regeneration in the Eastern Coasts of Ghana appears to have fundamentally
568 taken place during the previous decade. Essentially, mangrove vegetation appears to be
569 depleted before 2000 in Lake Songaw Lagoon where we only observe a few spots of this
570 vegetation by 2000. Most of this vegetation appears to have regenerated during the
571 previous decade. Mangrove area, which appears to have shrunk between the eastern part
572 of Volta Estuary and Keta Lagoon during the previous decade, appears to have increased
573 over the last decade. In contrast, mangrove vegetation appears to be in progressive decline
574 over the study period in Volta River and the western part of Volta Estuary where some
575 areas remained stable since 2000.

576 5. Discussion

577 The approach we presented addresses key issue related to optical remote sensing,
578 LUCC classification, and post-classification change detection. By reconstructing gap free
579 times series at the nominal spatial resolution in a context of persistent cloud cover, the

approach presents clear advantage for a wide range of remote sensing applications. On the one hand, the high classification accuracy we have achieved, despite a high number of LULC classes and validation samples, results from the ability of the approach to account for the history of pixels without accounting for random noise. On the other hand, the use of unsupervised classification to constrain the reference data over pixels of persistent LULC have contributed to this high accuracy. This approach can be almost always useful for remote sensing-based analysis, particularly in situations of limited resources and limited access to study sites. One limitation can be expected for pixels that undergone LULC change over a reference period for it can be confusing to which LULC it would be classified ([Zhu and Woodcock, 2014](#)). Obviously, this has not been of major concern in this study and is unlikely to constitute a problem as long as the reference period is wisely chosen. With a short and odd number of years as reference periods (i.e., 3 successive years) in our case, the distribution of any changed pixel would be skewed towards of the most likely characteristic LULC class. The random forest algorithm can then handle such situation without any ambiguity, particularly when the images in the time series are spread across multiple bands. In any case, the reference period should be chosen in a way to avoid capturing multiple changes while allowing the time series to capture enough data for the classification algorithm to find windows for discriminating pixels of different classes.

In the coastal regions of Ghana, the chance of getting clear Landsat observation appears to increase eastwards ([Figure 1](#)). From the result of mangrove dynamics, it becomes clear that the ability of the model to remove random noise depend on the amount of available clear observations. This is reflected by the presence of potentially noisy pixels in some of the change maps (i.e., Amansuri Lake, Kpani River, Butre Estuary) presented in [Figure 6](#). This noise decreases in space form West to East as more clear observations become available. It also decreases in time from the earliest to the most recent change map as more data become available with the availability of different Landsat sensors. One way to reduce this noise is to use the model by-products (e.g., phase and amplitude, harmonic coefficients) described in [equation \(1\)](#) as part of the classification inputs. Future works may

609 also consider the use of normalized difference spectral indices (e.g., NDVI, NDWI) along
610 with these model by-products to improve the estimates. With a few caveats, the increasing
611 availability of synthetic aperture radar data presents another opportunity to improve
612 these estimates. PALSAR-2/PALSAR (as yearly mosaic since 2007) and Sentinel-1 (as 12
613 days temporal resolution since 2015) data are currently freely available for Ghana from
614 Google Earth Engine.

615 The results of mangrove dynamics expose the major mangrove areas of Ghana, each
616 of which having its own peculiarity. In Ghana, it seems that mangrove degradation was
617 perceptible long before 2000 and has triggered a massive replanting campaign along the
618 coast. This led to the formation of organized groups engaged in systematic planting
619 and harvesting of mangrove trees. While regeneration of mangroves in most areas is
620 due to replanting, the causes of their degradation is more context specific even though
621 they mostly relate to overexploitation. Despite the noticeable impacts of the replanting
622 projects in many areas along the coast of Ghana, genuine support from local community
623 towards these projects has remained largely unclear ([Aheto et al., 2016](#); [Asante et al.,
624 2017](#)).

625 The spatial distribution of gain and loss in mangrove vegetation in Butre River suggests
626 a possible increase of salinity in the lower tributary since mangroves regeneration appear
627 to increase with lower order tributaries. Regardless the cause, the pattern of loss and
628 gain paints some sort of mangrove migration from the lower part to the upper part of
629 the river. This is likely to result into an overall decrease of mangrove vegetation in the
630 area since the potential area for mangrove development is higher in the lower basin. In
631 urban areas (e.g., Takoradi, Accra), the main drivers of mangrove degradation are urban
632 encroachment and pollution. The general pattern of mangrove degradation in these urban
633 centres relates to population density in relation to the carrying capacity of the mangrove
634 area, as in the case of Takoradi and Ayensu River. The closer the mangrove area to
635 settlement, the more likely the degradation, and the larger the agglomeration, the more
636 likely the degradation. The depletion of mangrove in Muni Lagoon, for instance, can
637 be mainly explained by the range of mangrove exploitation in relation to the carrying

capacity of the mangrove. In this area, mangroves were intensively used as source of domestic and commercial charcoal and firewood while being subjected to other practices (e.g., bush burning, agricultural encroachment, unsuitable fishing) that are conducive to their degradation ([A Rocha Ghana, 2016](#)). In Densu River, mangrove degradation is mainly due to increase urbanisation which resulted in the encroachment of mangrove areas, the dumping of waste into the river along with excessive fishing and oysters harvesting. In Volta Estuary, mangrove degradation stemmed from uncontrolled access to mangrove resources but the failure of mangrove restoration programmes is mainly due to issues related to governance and tenure along with the local perception of mangroves as a mean for economic gain rather than a mean for environmental conservation ([Asante et al., 2017](#); [Ashiagbor et al., 2021](#)).

In a nutshell, we identified 5 major groups of factors involved in mangrove degradation in Ghana.

1. Global changes including infrastructural development, urbanization and climate change. For example, the construction of the Akosombo dam of the Volta river negatively affected the agricultural and fishery sectors in the Volta estuary, resulting in increased cutting of mangroves by the local to make a living ([Aheto et al., 2016](#); [Feka and Ajonina, 2011](#); [Rubin et al., 1999](#)). Increased level of industrial and domestic wastes due to urbanization generally results in the pollution of water sources near cities. This is the case of Korle Lagoon which drains most of the untreated waste of Accra into Atlantic Ocean. This pollution, causing the proliferation of invasive species, the reduction of oxygen level and increasing the level of salinity, is particularly a problem for mangrove trees in Korle Lagoon ([Boadi and Kuitunen, 2002](#)).
2. Local awareness including local perceptions and the erosion of cultural and religious beliefs associated with coastal resources. Such examples are the cases of out-of-taboo fishing in Fosu, Muni and Songor lagoons ([Darkwa and Smardon, 2010](#); [Ntiamoa-Baidu, 1991](#)), the perception that the mangroves of Fosu Lagoon shelter dangerous species such as snakes ([Darkwa and Smardon, 2010](#)), or the drainage of urban waste

- 667 into mangroves swamps in Accra ([Essumang et al., 2012](#)).
- 668 3. Land tenure regime including the sense of ownership. Mangroves lease often goes
669 for a period of 10 years, resulting in increased tree cutting by the lessee ([Armah](#)
670 [et al., 2009](#)).
- 671 4. Legislation, governance and policy including the lack of enforcement for mangrove
672 resource protection [[Armah et al. \(2009\)](#); Feka-2015]. Despite the various conserva-
673 tion projects tailored to mangroves ecosystems in Ghana, these mangroves remain
674 vulnerable to anthropogenic disturbance as they lack a clear legislation that could
675 protect them from overexploitation ([Asante et al., 2017](#)).
- 676 5. Lucrative including commercial wood cutting, agricultural expansion or salt mining.
677 Examples of such are the conversion of mangroves into salt pans and urban encroach-
678 ment in Keta Lagoon ([Asante et al., 2017](#)), charcoal and firewood for fish smoking
679 in Fosu Lagoon ([Darkwa and Smardon, 2010](#)). [Aheto et al. \(2016\)](#) estimated the an-
680 nual net income per hectare of mangrove wood to approximate \$4824.88 for traders
681 and \$383.12 for planters.
- 682 Further study on the nexus between people and their mangrove across the whole coun-
683 try would provide interesting insights for conservation policies. Mangrove restoration can
684 be expansive as it does not only require the replanting of thousands of mangroves trees but
685 more importantly their maintenance and reaching thousands of people. The key aspect to
686 keep in mind is that mangroves degrade more as result as a lack of environmental educa-
687 tion (e.g., awareness of common resource and conservation issue, and strong management
688 skill at a general public level) than they do due to natural factors. Mangrove restoration
689 would require, in the first place, a large-scale training of the locals on sustainable use
690 and management of the mangrove. Amongst other things, mangrove restoration in Muni
691 required the inclusion of all communities (e.g., Mankoadze, Biwadze and Akosua Village)
692 whose activities impact the mangrove, a number of training sessions including, tree nurs-
693 ery as a mean to avail mangrove seedlings, mangrove management and conservation to
694 strengthen the local skill in mangrove planting and maintenance, the use and making of
695 efficient fuel stoves to reduce deforestation due to wood fuel.

696 Although the social dimension may be more crucial than the ecological one for man-
697 grove conservation, mangrove conservation policies should also consider the biophysical
698 settings in which mangroves evolve. Lagoons rely on water supplies from both the ocean
699 and some source of fresh water (e.g., rivers) which must be at an adequate proportion to
700 allow the development of certain mangrove species. It is important to keep the salinity at
701 a relatively low level, particularly for white mangrove such as Avicennia species. In this
702 case, alternative management model would consider a proper maintenance of fresh water
703 sources as a crucial aspect of management and conservation. An option of such manage-
704 ment would be river bank hedging. A hedgerow of tree along the river would protect the
705 river from erosion and sedimentation, and reduce evaporation to insure better fresh water
706 supply to the lagoon.

707 **Conclusion and recommendations**

708 This study addresses several issues concerning LULC classification, particularly when
709 the classification outputs are intended for LULC change detection. We discussed how
710 cloud cover can have important implications for LULC classification in the coastal re-
711 gions of Ghana and demonstrate how time series statistical models can be used to curate
712 this problem. Currently, Landsat mission is the best publicly available source of data that
713 provides sufficient records for studying decade-long LULC pathways in a comprehensive
714 manner. We argue that continuous time series analysis is more likely to provide unbi-
715 ased LULC classification than single point image analysis. Due to various remote sensing
716 artifacts, however, the temporal resolution of usable Landsat data is often insufficient
717 for continuous time series analysis. To address this challenge, our approach consisted in
718 capturing the inherent landscape phenology into time series statistical models that feed
719 on the few usable information to construct gap-free time series for image classification. In
720 regard to this issue, future research direction would be the use of both spatial and tem-
721 poral relationships between pixels to infer missing data. Such analysis should consider
722 harmonizing pixel level data such that these are comparable across spatial and temporal
723 domains. In this study, we discussed the issue of training data and classifiers, which need

724 to be comparable across the temporal scale of change detection analysis. While we have
725 not conducted formal analysis in regard to the effects of these aspects on our results, it ap-
726 pears that they have substantially contributed to the high statistical accuracy observed in
727 our classifications. Although the traditional confusion matrix provides formal estimate of
728 map accuracy in a variety of statistical metrics, studies dealing with LULC classification
729 should always cross-check the reliability of these metrics to ensure that maps reflect the
730 ground conditions. In this regards, future research direction would be the use of proba-
731 bilistic models to report class detection probabilities. Such exhaustive accuracy measures
732 would be more convenient and realistic in the sense that they estimate pixel-level accu-
733 racy, rather than class-level accuracy as does the traditional confusion matrix. Ecological
734 studies aiming at LULC classification and change detection can greatly benefits from the
735 use of continuous Landsat records and the other important considerations addressed in
736 this study. This can be particularly important when the signature of the target LULC
737 classes are similar. While mangroves represent our class of interest in this study, their
738 spectral signature is often similar to that of many forest LULC classes found in the study
739 area. This means that they can be easily mis-classified, in which case the classification
740 error would propagate into change detection. In such a case, the use of continuous time
741 series becomes a necessity rather than a luxury since it offers a rich data record for dis-
742 tinguishing between similar LULC via their phenological profiles. The analysis of LULC
743 dynamics show that LULC are subject of important conversion in the coastal regions of
744 Ghana. Future research directions would be to examine these LULC conversions. Such
745 studies may seek to understand which LULC are expanding, document which LULC are
746 shrinking as result of this expansion, estimate the rate at which the expansion is tak-
747 ing place, and investigate the main drivers of these LULC conversions. In this study,
748 we attempted to provide such information for mangrove vegetation and identify areas of
749 mangrove decrease and increase. Based on the results of our analysis, we recommend
750 large scale mangrove restauration in Ghana. Failure to do so is likely to result in the loss
751 of many mangrove areas, particularly those in the vicinity of urban centres. The first step
752 towards such a restauration program should be the zoning of priority areas, the quantifi-

753 cation of the costs and benefits in forms of spatially explicit ex-ante impact assessment,
754 and the definition of near and far futures milestones for mangrove development impacts.
755 Future research for mangrove changes analysis in the coastal regions of Ghana would be
756 the quantification of the change magnitude and the development of remote sensing-based
757 indicators of mangrove vegetation change and mangrove vegetation quality. In all these
758 cases, the use of spatially explicit statistical model capable of reconstruction high tempo-
759 ral frequency of comparable pixel data that accurately describe landscape-level phenology
760 of LULC provides a powerful tool for analysing changes in LULC.

761 Acknowledgements

762 This research was supported by the American People through the United States
763 Agency for International Development (USAID) under the BAA-AFR-SD-2020 Adden-
764 dum 01, (FAA No. 7200AA20FA00031). The contents of this manuscript are the sole
765 responsibility of the authors and do not necessarily reflect the views of USAID or the
766 United States Government.

767 References

- 768 A Rocha Ghana. Community mangrove restoration project, Muni Pomadze ramsar site. Technical
769 report, A Rocha Ghana, 2016. URL <https://ghana.arocha.org/projects/community-mangrove-restoration-project/>.
- 770
- 771 Bright Addae and Natascha Oppelt. Land-Use/Land-Cover Change Analysis and Urban Growth Mod-
772 elling in the Greater Accra Metropolitan Area (GAMA), Ghana. *Urban Science*, 3(1):26, feb 2019.
773 ISSN 2413-8851. doi: 10.3390/urbansci3010026. URL <http://www.mdpi.com/2413-8851/3/1/26>.
- 774 Denis Worlanyo Aheto, Stephen Kankam, Isaac Okyere, Emmanuel Mensah, Adams Osman,
775 Fredrick Ekow Jonah, and Justice Camillus Mensah. Community-based mangrove forest manage-
776 ment: Implications for local livelihoods and coastal resource conservation along the Volta estu-
777 ary catchment area of Ghana. *Ocean and Coastal Management*, 127, 2016. ISSN 09645691. doi:
778 10.1016/j.ocecoaman.2016.04.006.
- 779 G Ajonina, A Diamé, and J Kairo. Current status and conservation of mangroves in Africa: An overview.
780 *Journal of Chemical Information and Modeling*, 53(9):1689–1699, 2013. ISSN 1098-6596.
- 781 Aya Kojo Armah, George Wiafe, and David G. Kpelle. Sea-level rise and coastal biodiversity in West

- 782 Africa: A case study from Ghana. *Climate Change and Africa*, 9780521836:204–217, 2005. doi:
783 10.1017/CBO9780511535864.029.
- 784 Aya Kojo Armah, Abdoulaye Diame, Gordon Ajonina, and James Kairo. The role and work of African
785 Mangrove Network (AMN) in conservation and sustainable use of mangroves in Africa. *Nature &*
786 *Faune*, 24(1):30–41, 2009. URL <https://www.fao.org/3/ak995e/ak995e02.pdf>.
- 787 Winston A. Asante, Emmanuel Acheampong, Kyereh Boateng, and Jacob Adda. The implications
788 of land tenure and ownership regimes on sustainable mangrove management and conservation in
789 two Ramsar sites in Ghana. *Forest Policy and Economics*, 85(January):65–75, dec 2017. ISSN
790 13899341. doi: 10.1016/j.forepol.2017.08.018. URL <https://linkinghub.elsevier.com/retrieve/pii/S1389934117300370>.
- 791 George Ashiagbor, Winston Adams Asante, Jonathan Arthur Quaye-Ballard, Eric Kwabena Forkuo,
792 Emmanuel Acheampong, and Ernest Foli. Mangrove mapping using Sentinel-1 data for improved
793 decision support on sustainable conservation and restoration interventions in the Keta Lagoon Complex
794 Ramsar Site, Ghana. *Marine and Freshwater Research*, 2021. ISSN 1323-1650. doi: 10.1071/MF20105.
795 URL <http://www.publish.csiro.au/?paper=MF20105>.
- 796 Manson Awo, Akosua Boatema, Appoeing Addo Kwasi, and Adelina Mensah. Impacts of shoreline
797 morphological change and sea level rise on mangroves: the case of the keta coastal zone. *Journal of*
798 *Environmental Research and Management*, 4(11):0359–0367, 2014.
- 799 Cesar Aybar, Qiusheng Wu, Lesly Bautista, Roy Yali, and Antony Barja. rgee: An r package for
800 interacting with google earth engine. *Journal of Open Source Software*, 5(51):2272, 2020. doi:
801 10.21105/joss.02272. URL <https://doi.org/10.21105/joss.02272>.
- 802 Roger Bivand. classInt: Choose Univariate Class Intervals. Technical report, 2020. URL <https://cran.r-project.org/package=classInt>.
- 803 Kwasi Owusu Boadi and Markku Kuitunen. Urban waste pollution in the Korle Lagoon, Accra, Ghana.
804 *Environmentalist*, 22(4), 2002. ISSN 02511088. doi: 10.1023/A:1020706728569.
- 805 Leo Breiman. Random Forests. *Machine Learning*, 45(1):5–32, 2001. ISSN 1573-0565. doi: 10.1023/A:
806 1010933404324. URL <https://doi.org/10.1023/A:1010933404324>.
- 807 CILSS. *Landscapes of West Africa – A Window on a Changing World*. U.S. Geological Survey EROS,
808 47914 252nd St Garretson, SD 57030, 2016.
- 809 Sarah Darkwa and Richard Smardon. Ecosystem Restoration: Evaluating Local Knowledge and Man-
810 agement Systems of Fishermen in Fosu Lagoon, Ghana. *Environmental Practice*, 12(3):202–213, sep
811 2010. ISSN 1466-0466. doi: 10.1017/S1466046610000256. URL <https://www.tandfonline.com/doi/full/10.1017/S1466046610000256>.
- 812 Antonio Di Gregorio, Matieu Henry, Emily Donegan, Yelena Finegold, John Latham, Inge Jonckheere,
813 and Renato Cumani. *Land Cover Classification System: Classification concepts, Software version 3*.

- 817 FAO, Rome, Italy, 2016. ISBN 978-92-5-109017-6.
- 818 David K. Essumang, Louis K. Boampongsem, Christian K. Adokoh, John K. Bentum, Christiana
819 Owusu, Millicent E. Adu-Boakye, and Joseph Afrifa. Research Article: Evaluation of the Levels
820 of Selected Heavy Metals in Mangrove Ecosystem and Roadside Topsoil in Ghana. *Environmental*
821 *Practice*, 14(3):173–183, sep 2012. ISSN 1466-0466. doi: 10.1017/S1466046612000191. URL
822 <https://www.tandfonline.com/doi/full/10.1017/S1466046612000191>.
- 823 FAO. The world's mangroves 1980-2005. Technical report, FAO, Rome, Italy, 2007. URL <http://www.fao.org/3/a1427e/a1427e00.pdf>.
- 824 Njisuh Z. Feka and Gordon N. Ajonina. Drivers causing decline of mangrove in West-Central Africa:
825 a review. *International Journal of Biodiversity Science, Ecosystem Services & Management*, 7(3):
826 217–230, sep 2011. doi: 10.1080/21513732.2011.634436.
- 827 Zebedee Njisuh Feka. Sustainable management of mangrove forests in West Africa: A new pol-
828 icy perspective? *Ocean & Coastal Management*, 116:341–352, nov 2015. ISSN 09645691.
829 doi: 10.1016/j.ocecoaman.2015.08.006. URL <https://linkinghub.elsevier.com/retrieve/pii/S0964569115300053>.
- 830 FRA. Forest cover mapping and monitoring with NOAA - AVHRR and other coarse spatial resolution
831 sensors. Technical report, FAO, Rome, Italy, 2000. URL <http://www.fao.org/forestry/4031-0b6287f13b0c2adb3352c5ded18e491fd.pdf>.
- 832 Ghana Statistical Services. 2010 Population and Housing Census, final results. Technical report, Ghana
833 Statistical Service, 2012. URL http://statsghana.gov.gh/gsscommunity/adm_program/modules/downloads/get_file.php?file_id=27.
- 834 Noel Gorelick, Matt Hancher, Mike Dixon, Simon Ilyushchenko, David Thau, and Rebecca Moore. Google
835 Earth Engine: Planetary-scale geospatial analysis for everyone. *Remote Sensing of Environment*, 202
836 (1):18–27, dec 2017. ISSN 00344257. doi: 10.1016/j.rse.2017.06.031. URL <https://linkinghub.elsevier.com/retrieve/pii/S0034425717302900>.
- 837 Bin Jiang. Head/Tail Breaks: A New Classification Scheme for Data with a Heavy-Tailed Distribution.
838 *The Professional Geographer*, 65(3):482–494, aug 2013. ISSN 0033-0124. doi: 10.1080/00330124.2012.
839 700499. URL <http://www.tandfonline.com/doi/abs/10.1080/00330124.2012.700499>.
- 840 Eric F Lambin and Alan H Strahlers. Change-vector analysis in multitemporal space: A tool to detect
841 and categorize land-cover change processes using high temporal-resolution satellite data. *Remote*
842 *Sensing of Environment*, 48(2):231–244, may 1994. ISSN 00344257. doi: 10.1016/0034-4257(94)
843 90144-9. URL <https://www.sciencedirect.com/science/article/pii/0034425794901449https://linkinghub.elsevier.com/retrieve/pii/0034425794901449>.
- 844 Evan S. Levy, Noble K. Asare, Kobina Yankson, and Daniel A. Wubah. Effects of hydrographic conditions
845 of ponds on juvenile fish assemblages in the Kakum mangrove system, Ghana. *Regional Studies in*

- 852 *Marine Science*, 2:19–27, nov 2015. ISSN 23524855. doi: 10.1016/j.rsma.2015.08.007. URL <https://linkinghub.elsevier.com/retrieve/pii/S2352485515000390>.
- 853
- 854 Thomas Lillesand, Ralph W. Kiefer, and Jonathan Chipman. *Remote Sensing and Image Interpretation*.
855 John Wiley & Sons, 7th editio edition, 2015.
- 856 Y. Ntiamoa-Baidu. Conservation of coastal lagoons in Ghana: the traditional approach. *Landscape and*
857 *Urban Planning*, 20(1-3):41–46, jan 1991. ISSN 01692046. doi: 10.1016/0169-2046(91)90089-5. URL
858 <https://linkinghub.elsevier.com/retrieve/pii/0169204691900895>.
- 859 Thais Mayumi Oshiro, Pedro Santoro Perez, and José Augusto Baranauskas. How Many Trees in a
860 Random Forest? In Petra Perner, editor, *Machine Learning and Data Mining in Pattern Recognition*,
861 pages 154–168. Springer Berlin Heidelberg, Berlin, Heidelberg, 2012. ISBN 978-3-642-31537-4. doi: 10.
862 1007/978-3-642-31537-4_13. URL http://link.springer.com/10.1007/978-3-642-31537-4_13.
- 863 R Core Team. *R: A Language and Environment for Statistical Computing*. R Foundation for Statistical
864 Computing, Vienna, Austria, 2021. URL <https://www.R-project.org/>.
- 865 D.P. Roy, V. Kovalskyy, H.K. Zhang, E.F. Vermote, L. Yan, S.S. Kumar, and A. Egorov. Characterization
866 of Landsat-7 to Landsat-8 reflective wavelength and normalized difference vegetation index continuity.
867 *Remote Sensing of Environment*, 185:57–70, nov 2016. ISSN 00344257. doi: 10.1016/j.rse.2015.12.024.
868 URL <https://linkinghub.elsevier.com/retrieve/pii/S0034425715302455>.
- 869 J.A Rubin, C. Gordon, and J.K Amatekpor. Causes and Consequences of Mangrove Deforestation in
870 the Volta Estuary, Ghana: Some Recommendations for Ecosystem Rehabilitation. *Marine Pollution*
871 *Bulletin*, 37(8-12):441–449, dec 1999. ISSN 0025326X. doi: 10.1016/S0025-326X(99)00073-9. URL
872 <https://linkinghub.elsevier.com/retrieve/pii/S0025326X99000739>.
- 873 Mark Spalding, François Blasco, and Colin (Eds) Field. *World Mangrove Alias*. The International Society
874 for Mangrove Ecosystems, Okinawa, Japan, 1997.
- 875 Mark Spalding, Mami Kainuma, and Lorna Collins. *World Atlas of Mangroves*. Earthscan, London, UK,
876 2010.
- 877 UNEP. Mangroves of Western and Central Africa. Technical report, UNEP, Cambridge, UK, 2007. URL
878 <https://archive.org/download/mangrovesofweste07corc/mangrovesofweste07corc.pdf>.
- 879 USGS EROS. West Africa: Land Use and Land Cover Dynamics, 2021. URL <https://eros.usgs.gov/westafrica/mangrove#:~:text=Mangrovesplayanessentialrole,threatenedecosystemthroughouttherregion>.
- 880
- 881
- 882 Jan Verbesselt, Rob Hyndman, Glenn Newnham, and Darius Culvenor. Detecting trend and seasonal
883 changes in satellite image time series. *Remote Sensing of Environment*, 114(1):106–115, jan 2010. ISSN
884 00344257. doi: 10.1016/j.rse.2009.08.014. URL <https://linkinghub.elsevier.com/retrieve/pii/S003442570900265X>.
- 885
- 886 Le Wang, Mingming Jia, Dameng Yin, and Jinyan Tian. A review of remote sensing for mangrove

- 887 forests: 1956–2018. *Remote Sensing of Environment*, 231(December 2018):111223, sep 2019. ISSN
888 00344257. doi: 10.1016/j.rse.2019.111223. URL <https://linkinghub.elsevier.com/retrieve/pii/S0034425719302421>.
- 890 M L Wilkie and S Fortuna. Status and trends in mangrove area extent worldwide. Technical report,
891 FAO, Rome, Italy, 2003. URL <http://www.fao.org/3/j1533e/J1533E00.htm#TopOfPage>.
- 892 Michael A. Wulder, Thomas R. Loveland, David P. Roy, Christopher J. Crawford, Jeffrey G. Masek,
893 Curtis E. Woodcock, Richard G. Allen, Martha C. Anderson, Alan S. Belward, Warren B. Cohen, John
894 Dwyer, Angela Erb, Feng Gao, Patrick Griffiths, Dennis Helder, Txomin Hermosilla, James D. Hipple,
895 Patrick Hostert, M. Joseph Hughes, Justin Huntington, David M. Johnson, Robert Kennedy, Ayse
896 Kilic, Zhan Li, Leo Lymburner, Joel McCorkel, Nima Pahlevan, Theodore A. Scambos, Crystal Schaaf,
897 John R. Schott, Yongwei Sheng, James Storey, Eric Vermote, James Vogelmann, Joanne C. White,
898 Randolph H. Wynne, and Zhe Zhu. Current status of Landsat program, science, and applications.
899 *Remote Sensing of Environment*, 225:127–147, may 2019. ISSN 00344257. doi: 10.1016/j.rse.2019.02.
900 015. URL <https://linkinghub.elsevier.com/retrieve/pii/S0034425719300707>.
- 901 Zhe Zhu and Curtis E. Woodcock. Continuous change detection and classification of land cover us-
902 ing all available Landsat data. *Remote Sensing of Environment*, 144:152–171, mar 2014. ISSN
903 00344257. doi: 10.1016/j.rse.2014.01.011. URL <https://linkinghub.elsevier.com/retrieve/pii/S0034425714000248>.
- 904 Zhe Zhu, Shixiong Wang, and Curtis E. Woodcock. Improvement and expansion of the Fmask algorithm:
905 cloud, cloud shadow, and snow detection for Landsats 4–7, 8, and Sentinel 2 images. *Remote Sensing
906 of Environment*, 159:269–277, mar 2015. ISSN 00344257. doi: 10.1016/j.rse.2014.12.014. URL <https://linkinghub.elsevier.com/retrieve/pii/S0034425714005069>.